NIH Public Access
Author Manuscript
Nano Lett. Author manuscript; available in PMC 2014 May 14.

Published in final edited form as:
Nano Lett. 2009 September ; 9(9): 3337–3342. doi:10.1021/nl901610f.

A High Performance Nano-Bio Photocatalyst for Targeted Brain Cancer Therapy

Elena A. Rozhkova[1,*], **Ilya Ulasov**[2], **Barry Lai**[3], **Nada M. Dimitrijevic**[1,4], **Maciej Lesniak**[2], and **Tijana Rajh**[1]

[1]The Center for Nanoscale Materials, Argonne National Laboratory, Argonne, IL 60439, USA

[2]The University of Chicago Brain Tumor Center, the University of Chicago, Chicago, IL 60637

[3]The Advanced Photon Source, Argonne National Laboratory, Argonne, IL 60439, USA

[4]Chemical Sciences and Engineering Division Argonne National Laboratory, Argonne, IL 60439, USA

Abstract

We report pronounced and specific anti-glioblastoma cell phototoxicity of 5 nm TiO_2 particles covalently tethered to an antibody via dihydroxybenzene bivalent linker. The linker application enables absorption of a *visible* part of solar spectrum by the nanobio hybrid. The phototoxicity is mediated by reactive oxygen species (ROS) that initiate cancer cell programmed cell death. Synchrotron X-Ray Fluorescence Microscopy (XFM) was applied for direct visualization of the nanobioconjugate distribution through a single brain cancer cell at the sub-micrometer scale.

The vibrant development of modern nanotechnology and nano-biotechnology opens novel horizons for diagnosis, imaging, and therapy of diseases that have traditionally been recognized as incurable via basic therapies or surgical methods. Malignant glioma, in particular glioblastoma multiforme (GBM), represents a devastating form of primary brain cancer characterized by resistance to conventional adjuvant therapies. Despite surgery, radiation and chemotherapy treatments the median survival is measured in months rather than years. [1–2] Cases of primary malignant brain and other nervous system tumors were estimated at ~23,000 annually, and about 13,000 people die of malignant brain tumors each year in the United States.[3] In light of this prognosis, innovative adjuvant technologies include gene-, immuno-therapy, and nanotechnology platforms. The ability to integrate the advanced properties of nanoscaled materials with the unique recognition capability of biomolecules to achieve active transport, imaging and, finally, specific elimination of malignancies makes emerging nanoplatforms attractive for the development of rationally designed modalities for neuro-oncology.[4] Semiconductor TiO_2 is well-known as a photocatalyst in the degradation of organic substrates [5] and the deactivation of

[*]Corresponding author: rozhkova@anl.gov.

Supporting information available: Supporting Information is provided to describe detailed materials and methods. We describe the TiO_2-antibody conjugates synthesis and characterization, the cell lines along with culture conditions, ELISA protocol, pohoto-induced cytotoxicity and cell viability examination set-up, histo-immunochemical analysis of apoptosis by fluorescent confocal microscopy, X-ray fluorescence Microprobe Elemental Analysis Spectrum and statistics used. This material is available free of charge via the Internet at:

NIH-PA Author Manuscript
NIH-PA Author Manuscript
NIH-PA Author Manuscript

NIH-PA Author Manuscript

NIH-PA Author Manuscript

NIH-PA Author Manuscript

microorganisms [6–11] and viruses. [12] Under ultraviolet light (UV) excitation, TiO_2 nanoparticles of various sizes and morphologies have been reported to exhibit cytotoxicity toward some tumors. [13–22] Although nanomaterials tend to passively accumulate in tumors due to the so-called enhanced "permeability and retention effect" and often serve as a "nanocarriers" for chemotherapeutics, this passive strategy has limitations due to its random delivery mode. [23] In this work we propose a technique to overcome the passive transport drawbacks by integrating the hard inorganic nanomaterial with a biological soft material, an antibody which is able to recognize the GBM cells. The interleukin-13α2 receptor domain (IL13α2R) has been widely studied due to its importance in tumor biology. [24] It binds to interleukin-13 (IL13), a key signaling molecule in malignancy and inflammation, with consequent internalization of the ligand-receptor complex inside the tumor cell. [25–27] The IL13α2R has been reported to be exclusively over-expressed on the surface of certain tumors, including GBM. [28–30] Therefore the IL13α2R is an ideal candidate to serve as a marker and a glioma-targeting vehicle for cytotoxic elements, such as toxins [28], virus [31] and immunonanoshells. [32] We focus on the development of a polychromatic visible-light inducible nano-bio hybrid system based on the 5 nm TiO_2 nanocrystals covalently tethered to a biological vehicle capable of selective recognition of the GBM, Figure 1. Like the Photodynamic Therapy (PDT) our approach includes three main components: light, oxygen and a photoreactive material. The hybrid semiconductor particles absorb energy from light which is then transferred to molecular oxygen, producing cytotoxic reactive oxygen species (ROS). While brain tumors can not be exposed to light directly, even the deepest brain tumors may become accessible during surgery, and light-based techniques may serve as an excellent intraoperative adjuvant therapy.[4] The advantages of nanoscale photosensitizes to compare to "classical" PDT are the result of synergistic combination of advanced physical properties of inorganic materials with targeting abilities of biomolecules and the multiple functions of drugs and imaging payloads in one ideal therapeutic system.[33] Furthermore, nanoparticles may overcome biological barriers, including BBB. [33]

TiO_2-mAb photocatalyst synthesis, characterization and bio-recognition functionality assay

Initially, we synthesized 5 nm TiO_2 nanoparticles in accordance with previous reports. [34] The particles were capped with 1,2-Epoxy-3-isopropoxypropane (glycidyl isopropyl ether) to prevent undesirable reactions of hydroxyl groups at the TiO_2 surface with biomolecules or cell membranes. The capped particles were covalently conjugated with the IL13α2R-targeting antibody (anti-human-IL13α2R, hereafter referred as mAb) through amide linkage via a bidentate surface linker under conditions selected to retain both the immune reactivity and the photocatalytic activity of the final TiO_2-mAb conjugates. Approaches for tethering biomolecules to the surface of TiO_2 particles utilize the ability of oxygen-containing functional groups, such as carboxy-, hydroxyl-, and phosphate, to bind to the surface of nanoparticles. [35–37] Our strategy to construct bio-TiO_2 hybrids is based on dihydroxybenzenes, for example dopamine (DA), as linkers. Due to the presence of two OH- groups in the ortho- position, catecholate group forms a strong bidentate complex with coordinatively unsaturated Ti atoms at the surface of nanoparticles. [36] Furthermore, it has been shown that when DNA or proteins are covalently bound to DA, DA acts as a

NIH-PA Author Manuscript

NIH-PA Author Manuscript

NIH-PA Author Manuscript

conductive bridge between TiO_2 biomolecules and nanocrystals allowing transport of photogenerated holes to the biomolecules. [38–39] In this study, we used another dihydroxybenzene linker, a naturally-occurring metabolite of dopamine – 3,4-dihydroxyphenilacetic acid (DOPAC). Similar to dopamine, the ene-diol containing bivalent linker DOPAC simultaneously serves two key functions. First, chemisorption of DOPAC "heals" the semiconductor surface enhancing and optimizing the nanocrystal exterior charge-transfer dynamics enabling absorption of a *visible* part of solar spectrum. Second, DOPAC chemisorption modifies the particle surface with carboxylic functional groups, which are useful for further covalent tethering to a biomolecule. After instant chemisorption of DOPAC on the nanoparticles surface (using 100 times excess), the resulting carboxylic groups of the TiO_2-DOPAC particles were pre-activated using Sulfo-NHS/EDAC, and then coupled to aminogroups of mAb via carbodiimide chemistry. The final product, TiO_2-DOPAC-anti-IL13α2R (hereafter referred as TiO_2-mAb), was purified and characterized. Next, we tested whether the mAb retains its recognition activity after tethering to the TiO_2 particles by the standard ELISA technique. The binding affinity was determined to be comparable to that of unconjugated antibody (Figure S2-A). Some reduction (up to 10%) of a conjugated antibody activity can originate from steric hindrances due to the nanoparticles attachment, or possibly by partial blockage of mAb recognition sites. The both conjugated and unconjugated mAb showed binding affinity with A172 high- and U87MG low-IL13α2R expressing human GBM cell lines (Figures S2-B and C). In contrast, isotypical immunoglobulin IgG1, either conjugated or unconjugated, did not recognize isolated or cellular IL13α2R. In cell experiments, TiO_2-mAb binding profiles depended on the level of IL13α2R expression. On average, concentrations of unconjugated or conjugated mAb under ~1 μg/ml responded to the antigen linearly, and data for concentrations above 1 μg/ml indicated saturation. For this reason, for both high- and low- IL13α2R expressing cells, we chose 6–600 ng/ml of the conjugate as an average working concentration for subsequent toxicity studies.

X-ray Fluorescence Microscopy single cell imaging

To obtain direct visualization of the ligand-receptor interaction and map the location and distribution of specific human GBM receptors throughout a single brain cancer cell we utilized X-ray Fluorescence Microscopy (XFM) using the *Advanced Photon Source* (APS). Third-generation synchrotrons with spatially coherent high-brilliance X-rays allow elemental mapping of biological specimens in near-native environments with sub-micron spatial resolution, which provides valuable complementary information to visible light microscopy. Thus, XFM has been proven to be a powerful technique for the analysis of metals distribution within single bacterial or mammalian cell or cellular compartments. [40–42]

We used A172 cells as a model for the XFM studies due to their high IL13α2R expression. An incident X-ray beam of 10 keV energy was used to excite elements from silicon to zinc which have x-ray emission lines in the 1–10 keV regime, Figure S3. As shown in Figure 2, XFM revealed that titanium is distributed throughout the entire membrane of an A172 glioma cell. Higher titanium signals were detected at the cell, as shown in Figure S3, Supporting Information. This is expected based upon the sample preparation technique. An additional important finding which resulted from the XFM study is that the specialized

NIH-PA Author Manuscript

NIH-PA Author Manuscript

NIH-PA Author Manuscript

subcellular structures *invadopodia* are also covered by the TiO_2-mAb (Figure 2, bottom). Invasiveness of diseased cells is one hallmark of GBM. Invadopodia, or invasive foot processes, are actin-rich micron-scale protrusions observed in some malignant cells, including head and neck squamous cell carcinoma, breast carcinoma, melanoma, and glioma, that assault surrounding healthy tissue. [43] Visualization and controlled disruption of this dynamic cytoarchitectural element is an important step toward development of novel anti-invasive therapies and cancer diagnostics. In addition, the presence of IL13α2R on GBM subcellular structures emphasizes once more that this specific receptor is an important antigen for advanced targeted anti-GBM therapies. Although "post"-fixation interaction of the cellular membrane antigen with TiO_2-mAb did not permit visualization of some intriguing events (e.g. the possible internalization of the nanobioconjugate facilitated by the IL13α2R subunit), the following important inferences from the present XFM studies can be drawn: i) the mAb covalently tethered to the TiO_2 particles serves as a biological vehicle carrying the nanoconjugate to the target - the GBM cell; ii) although only very low concentrations of the bio-nanoconjugate were applied, active antibody-assisted targeting achieved detectable local concentrations of the titanium comparable to concentrations of biogenic elements such as Zn at the outer cell membrane, (Figures 2 and S3); iii) nano-sized metal-organic materials containing non-biogenic metals, such as Ti, Au, Ag, and others tethered to an IL13α2R-recognising antibody, are excellent candidates for development of a novel generation of nano-tags for XFM-based diagnostic assays useful to evaluate tumor initiation and progression.

Photo-induced TiO_2-mAb cytotoxicity toward GMB

As highlighted herein, TiO_2 nano-materials of various sizes, morphology, and solubility have been suggested to destroy certain cancer cells. However, because it is a semiconductor with a relatively large band-gap of 3.2 eV, TiO_2 is activated only by UV light of wavelengths shorter than about 380 nm. Modification of TiO_2 particles with electron donating ene-diol ligands results in significant improvement to the outer crystal structure and photoreactivity of the particles, narrowing the band-gap to 1.6 eV and red-shifting the absorption edge to the visible part of the solar spectrum below ~750 nm. [44] For example, extinction coefficients for the absorption of TiO_2/Dopamine complexes were determined to be 3.3×10^3 M^{-1} cm^{-1} at 440 nm, 1.1 $x10^3$ M^{-1} cm^{-1} at 520 nm, and 1.0×10^2 M^{-1} cm^{-1} at 570 nm. [38, 44] As a result, catecholate-modified TiO_2 nanoparticles exhibit promising properties for biomedical applications because of the optimal spectral window for biological tissue penetration is around 800 nm to 1 μm. We examined TiO_2-mAb conjugates in cytotoxicity experiments induced by polychromatic visible light by assaying the loss of cell membrane integrity based upon the release of cellular lactate dehydrogenase (LDH) into a medium. Three cell lines: A172, U87 and normal human astrocytes (NHA), were tested. Cells were incubated with the nanobioconjugate for 1 hour, then washed thoroughly and exposed to focused polychromatic visible light for 5 minutes. Optical (400 nm cut-off) and water filters were used to insure that cytotoxicity was not the result of UV exposure or IR-induced hyperthermia. In all experiments, the cell culture solution temperature was remotely monitored with an infrared camera. When water filter was applied during the light exposure, the culture buffer temperature increased by ~1 degree only (from 24.45 to 25.61°C), while

NIH-PA Author Manuscript

NIH-PA Author Manuscript

NIH-PA Author Manuscript

without the filter the temperature raised ~6–7 degrees. This excludes hyperthermia as a possible mechanism of cell damage. Additionally, cells without nanoparticles were also exposed to the focused light and used as a background control to estimate the nanoparticles-driven phototoxicity. After light exposure, these cells were incubated in standard conditions for recovery and LDH release was tested after 6, 24 and 48 hours according to the manufacturer's protocol. As summarized in Figure 3, neither TiO_2 nor TiO_2-mAb was toxic in the dark. In contrast, light-induced TiO_2-mAb in concentrations ranging from 6 to 600 ng/ml exhibited pronounced light-induced cytotoxicity toward both A172 and U87 cells, moreover, even after 48 hours after exposure to light toxicity was still high (Figure 3 A and B; 24-hour time data was omitted for a figure clarity). Notably, in the case of A172 cells with high IL13α2R overexpression, the toxicity had a concentration-dependent character and reached its maximum of 80% 6 hours after exposure to light, whereas the photo-induced toxicity toward U87 cells with low receptor-expression reached a plateau around ~50% and did not change significantly with increasing nanoconjugate concentration. This observation correlates well with prior binding experiments, and can be explained assuming saturation of all vacant IL13α2 receptors on U87 cells by the lower concentrations of the conjugate. It should be pointed out that TiO_2 particles tethered to the isotypical immunoglobulin were unable to recognize IL13α2R and did not show notable cytotoxicity, as shown in Figure 3, A and B. It is also significant that TiO_2-mAb conjugate did not show cytotoxicity toward NHA, Figure 3C. Passive transport of free TiO_2 nanoparticles resulted in some light-induced cytotoxicity (maximum ~15%) for all cells tested; see Figure 3 A, B and C.. This fact clearly demonstrates the benefits of precisely-controlled active transport of nanoparticles to the target cells in contrast to passive nanomaterial-cancer cell interfacing.

Detection of ROS involved in the cytotoxicity

It is well established that UV-photoexcitation of TiO_2 in an aqueous solution results in the formation of the various reactive oxygen species such as hydroxyl (OH), and peroxy (HO_2) radicals, superoxide anions (O_2^-), hydrogen peroxide (H_2O_2) and singlet oxygen ($^1O_2$). [45–49] Recently, using the spin-trap EPR and radical-induced fluorescence techniques we have demonstrated that formation of ROS arises from mechanically distinct multiple redox chemistries on the surface of dopamine-modified and bare TiO_2 particles. [50] The major ROS produced upon illumination of TiO_2/DA or TiO_2 linked to a biomolecule through a DA bridge detected was the superoxide anion, formed by reaction of photogenerated electrons with molecular oxygen while the measured yield of $^1O_2$ was very low compared to bare TiO_2. [50] In this study, we investigated whether the observed cytotoxicity was mediated by photo-induced generation of ROS and whether our previous "pure" physicochemical *in vitro* and cellular *in situ* studies are consistent We found that cellular LDH release was remarkably inhibited by 10 unit/ml superoxide dismutase SOD (superoxide natural scavenger), or 2 mM sodium azide (singlet oxygen and OH· trap), somewhat less inhibited by 100 unit/ml catalase (quencher of hydrogen peroxide), and only partially suppressed by 50 mM mannitol (a quencher of hydroxyl radicals), as shown in Figure 3D. Unlike sodium azide, histidine (another singlet oxygen quencher) only inhibited the cytotoxicity moderately, (refer to Figure 3D). The higher efficiency of azide in singlet oxygen quenching probably arises from its large rate constant, which in vitro is two orders

NIH-PA Author Manuscript

NIH-PA Author Manuscript

NIH-PA Author Manuscript

of magnitude higher than for histidine. [51] These results suggest that under illumination with visible light, the photo-induced cytotoxicity of TiO_2 tethered to mAb through a DOPAC linker is mediated by oxygen-centered active radicals. Taking into account our recent EPR studies [50] and the results of current cell toxicity experiments, we believe that the superoxide anion is the primary ROS responsible for cell membrane damage, permeability changes, and cell death. Further radical reactions of superoxide can lead to singlet oxygen, hydrogen peroxide, and hydroxyl radical formation.

Evidence of apoptosis

Identification of the ROS involved in the light-induced toxicity is important because it reveals mechanisms of cell death allowing rational development of cancer therapeutics. The formation of relatively short-lived (nanoseconds) ROS with relatively low diffusion lengths, e.g. hydroxyl radicals (< 20 nm) and singlet oxygen, (20–220 nm in a cell) can result in necrosis. [52–53] On the other hand, ROS with longer half-lifetimes (milliseconds), such as O_2-/HO_2 and H_2O_2, are able to reach cell organelles, first of all mitochondria, to alter electron transfer respiratory pathways and promote apoptosis. Since we propose that the major ROS produced by photo-excited TiO_2-mAb is superoxide, we investigated possible changes to cellular membranes, namely the membrane symmetry, associated with apoptosis. Viable cells maintain an asymmetric distribution of phospholipids between the outer and inner part of plasma membranes. Apoptic changes are specifically characterized by the loss of *intact* phospholipid membrane asymmetry and inversion of the cytosol-facing lipid phosphatidyl serine (PS) at the outer side of the membrane, as shown in Figure 4. Exposed PS is recognized by phagocytes for subsequent inflammation-free physiological elimination. In our experiments, PS was detected via reaction with fluorescein-labeled Annexin V and laser-confocal microscopy imaging. As shown in Figure 4, typical apoptotic loss of membrane asymmetry was observed only in the case of photo-induced TiO_2-anti-mAb. No indication of the cell membrane inversion was detected for unconjugated TiO_2 particles or the non-specific TiO_2-IgG1 conjugate. Taking into account that other ROS, including primary and secondary radicals, can be generated by photo-induced TiO_2-mAb, it is most likely that the observed GBM cells death is a multistep process and, depending upon "spatially-resolved" cellular response, may involve other types of programmed cells death, including necrotic- and autophagic-type pathways.

In summary, our results show the first evidence of successful bio-conjugated nanoparticles targeting toward cancer and away from normal brain cells. We utilized a platform of 5 nm TiO_2 nanoparticles tethered through a DOPAC linker to the anti-human-IL13α2R. These data support the following model for the visible light-induced phototoxicity of the TiO_2-nanobio hybrid toward human brain cancer: induced by visible light: the functionally-integrated nanosized TiO_2/antibody complex retains both its biorecognition ability and its photoreactivity; the nanobiocomposite binds exclusively to GBM cells and, under exposure to *visible light*, initiates the production of ROS, which damages the cell membrane and induces programmed death of the cancer cell (Figure 1). Equally significant, for first time we report the direct visualization of ligand-receptor interactions and mapping of a specific human GBM receptor through a single brain cancer cell using TiO_2 nanoparticles through XFM hard X-rays of the APS.

NIH-PA Author Manuscript

NIH-PA Author Manuscript

NIH-PA Author Manuscript

Supplementary Material

Refer to Web version on PubMed Central for supplementary material.

Acknowledgments

The work was performed under the auspices of the U.S. Department of Energy, Office of Basic Energy Sciences under Contract No. DE-AC02-06CH11357. Support by the National Cancer Institute (R01-CA122930, R21-CA135728 MSL), the National Institute of Neurological Disorders and Stroke (K08-NS046430, MSL), the Alliance for Cancer Gene Therapy Young Investigator Award (MSL), the American Cancer Society (RSG-07-276-01-MGO, MSL) and Brain Research Foundation (Award FAS # 6-33186 to ER) is gratefully acknowledged. The authors thank Dr. L. Finney (APS, ANL), Dr. S. Vogt (APS, ANL) and Dr. J. Maser (CNM, ANL) for valuable discussions and technical advising in XFM samples preparation, Dr. D.-H. Kim (Material Science Division, ANL) for assistance with FT-IR spectroscopy, Dr. V. Novosad (MSD, ANL) for AFM imaging and G. Ms. Shustakova (MSD, ANL) for assistance with infrared camera thermal imaging. We thank Dr. A. Datesman for reading the manuscript.

References

1. Lesniak MS, Brem H. Nat Rev Drug Discover. 2004; 3:499–508.
2. Stupp R, Weber DC. Onkologie. 2005; 28:315–317. [PubMed: 15933418]
3. National Cancer Institute, Surveillance Epidemiology and End Results, SEER; http://seer.cancer.gov/statfacts/html/brain.html#ref10
4. Koo YEL, Reddy GR, Bhojani M, Schneider R, Philbert MA, Rehemtulla A, Ross BD, Kopelman R. Advanced Drug Delivery Reviews. 2006; 58:1556–1577. [PubMed: 17107738] Orringer DA, Koo YE, Chen T, Kopelman R, Sagher O, Philbert MA. CLINICAL PHARMACOLOGY & THERAPEUTICS. 2009; 85:531–534. and references wherein. [PubMed: 19242401]
5. Szaciowski K, Macyk W, Drzewiecka-Matuszek A, Brindell M, Stochel G. Chem Rev. 2005; 105:2647–2694. [PubMed: 15941225]
6. Sunada K, Watanabe T, Hashimoto K. J Photochem Photobiol A-Chem. 2003; 156:227–233.
7. Sokmen M, Candan F, Sumer Z. J Photochem Photobiol A-Chem. 2001; 143:241–244.
8. Theron J, Walker JA, Cloete TE. Critical Rev Microbiol. 2008; 34:43–69. [PubMed: 18259980]
9. Amezaga-Madrid P, Nevarez-Moorillon GV, Orrantia-Borunda E, Miki-Yoshida M. FEMS Microbiol Lett. 2002; 211:183–188. [PubMed: 12076810]
10. Shah RR, Kaewgun S, Lee BI, et al. J Biomed Nanothech. 2008; 3:339–348.
11. Linkous CA, Carter GJ, Locuson DB, et al. Environ Sci Technol. 2000; 34:4754–4758.
12. Yamaguchi K, Sugiyama T, Kato S, et al. J Med Virol. 2008; 80:1322–1331. [PubMed: 18551617]
13. Cai R, Hashimoto K, Itoh K, et al. Bull Chem Soc Jp. 1991; 64:1268–1273.
14. Cai RX, Kubota Y, Shuin T, et al. Cancer Res. 1992; 52:2346–2348. [PubMed: 1559237]
15. Sakai H, Ito E, Cai, Yoshioka RX, et al. Biochim Biophys Acta. 1994; 1201:259–265. [PubMed: 7947940]
16. Kubota Y, Shuin T, Kawasaki C, et al. Br J Cancer. 1994; 70:1107–1111. [PubMed: 7981061]
17. Sakai H, Baba R, Hashimoto K, et al. Chem Lett. 1995; 3:185–186.
18. Lu PJ, Ho IC, Lee TC. Mutation Res-Gen Toxicol Envir Mutagenesis. 1998; 414:15–20.
19. Uchino T, Tokunaga H, Ando M, Utsumi H. Toxicol in Vitro. 2002; 16:629–635. [PubMed: 12206830]
20. Seo JW, Chung H, Kim MY, et al. SMALL. 2007; 3:850–853. [PubMed: 17385208]
21. Juan X, Yi S, Junjie H, Chunmei C, Guoyuan L, Yan J, Yaomin Z, Zhiyu J. Bioelectrochemistry. 2007; 71:217–222. [PubMed: 17643355]
22. Kalbacova M, Macak JM, Schmidt-Stein F, Mierke CT, Schmuki P. Physica Status Solidi - Rapid Research Letters. 2008; 2:194–196.
23. Peer D, Karp JM, Hong S, Faro K, Hzad OC, Margalit R, Langer R. Nature nanotechnology. 2007; 2:751–760.

NIH-PA Author Manuscript

NIH-PA Author Manuscript

NIH-PA Author Manuscript

24. Debinski W, Gibo DM. Mol Med. 2000; 6:440–449. [PubMed: 10952023]
25. Mintz A, Gibo DM, Slagle-Webb B, Christensen ND, Debinski W. NEOPLASIA. 2002; 4:388–399. [PubMed: 12192597]
26. Kawakami K, Taguchi J, Murata T, Puri RK. Blood. 2001; 97:2673–2679. [PubMed: 11313257]
27. Kawakami K, Takeshita F, Puri RK. J Biol Chem. 2001; 276:25114–25120. [PubMed: 11352909]
28. Debinski W, Gibo D, Hulet S, Connor J, Gillespie G. Cancer Res. 1999; 5:985–990.
29. Kawakami K, Kawakami M, Snoy PJ, Husain SR, Puri RK. J Exp Med. 2001; 194:1743–1754. [PubMed: 11748276]
30. Wykosky J, Gibo DM, Stanton C, Debinski W. Clin Canc Res. 2008; 14:199–208.
31. Zhou G, Yet GJ, Debinski W, Roizman B. Proc Natl Acad Sci USA. 2002; 99:15124–15129. [PubMed: 12417744]
32. Bernardi RJ, Lowery AR, Thompson PA, Blaney SM, West JL. J Neurooncol. 2008; 86:165–172. [PubMed: 17805488]
33. Ferrari M. Nature Rev Cancer. 2005; 5:161–171. [PubMed: 15738981]
34. Rajh T, Tiede DM, Thurnauer MC. J NON-CRYSTALLINE SOLIDS. 1996; 207:815–820.
35. O'Regan B, Gratzel M. Nature. 1991; 353:737–740.
36. Rajh T, Chen LX, Lukas K, Liu T, Thurnauer MC, Tiede DM. J Phys Chem B. 2002; 106:10543–10552.
37. Duncan WR, Prezhdo OV. Annu Rev Phys Chem. 2007; 58:143–184. [PubMed: 17059368]
38. Rajh T, Saponjic Z, Liu J, Dimitrijevic NM, Scherer NF, Vega-Arroyo M, Zapol P, Curtiss LA, Thurnauer MC. Nano Lett. 2004; 4:1017–1023.
39. Dimitrijevic NM, Saponjic ZV, Rabatic BM, Rajh T. J Am Chem Soc. 2005; 127:1344–1345. [PubMed: 15686345]
40. Kemner KM, Kelly SD, Lai B, Maser J, O'Loughlin EJ, Sholto-Douglas D, Cai ZH, Schneegurt MA, Kulpa CF, Nealson KH. Science. 2004; 306:686–687. [PubMed: 15499017]
41. Paunesku T, Rajh T, Wiederrecht G, Maser J, Vogt S, Stojicevic N, Protic M, Lai B, Oryhon J, Thurnauer M, Woloschak G. Nature Materials. 2003; 2:343–346.
42. Finney L, Mandava S, Ursos L, Zhang W, Rodi D, Vogt S, Legnini D, Maser J, Ikpatt F, Olopade OI, Glesne D. Proc Natl Acad Sci U S A. 2007; 104:2247–2252. [PubMed: 17283338]
43. Stylli SS, Kaye AH, Lock P. J of Clin Neuroscience. 2008; 15:725–737.
44. de la Garza L, Saponjic ZV, Dimitrijevic NM, Thurnauer MC, Rajh T. J Phys Chem B. 2006; 110:680–686. [PubMed: 16471588]
45. Hoffmann MR, Martin ST, Choi W, Bahnemann DW. Chem Rev. 1995; 95:69–96.
46. Mills A, Le Hunte S. J Photochem Photobiol A Chem. 1997; 108:1–35.
47. Schwarz PF, Turro NJ, Bossmann SH, Braun AM, Wahab AMAA, Durr H. J Phys Chem B. 1997; 101:7127–7134.
48. Daimon T, Nosaka Y. J Phys Chem C. 2007; 111:4420–4424.
49. Tachikawa T, Majima T. J Fluoresc. 2007; 17:727–738. [PubMed: 17453327]
50. Dimitrijevic NM, Rozhkova EA, Rajh T. J Am Chem Soc. 2009; 131:2893–2899. [PubMed: 19209860]
51. Basumodak S, Tyrrell RM. Canc Res. 1993; 53:4505–4510.
52. Redmond RW, Kochevar IE. Photochem Photobiol. 2006; 82:1178–1186. [PubMed: 16740059]
53. Schweitzer C, Schmidt R. Chem Rev. 2003; 103:1685–1757. [PubMed: 12744692]

NIH-PA Author Manuscript
NIH-PA Author Manuscript
NIH-PA Author Manuscript

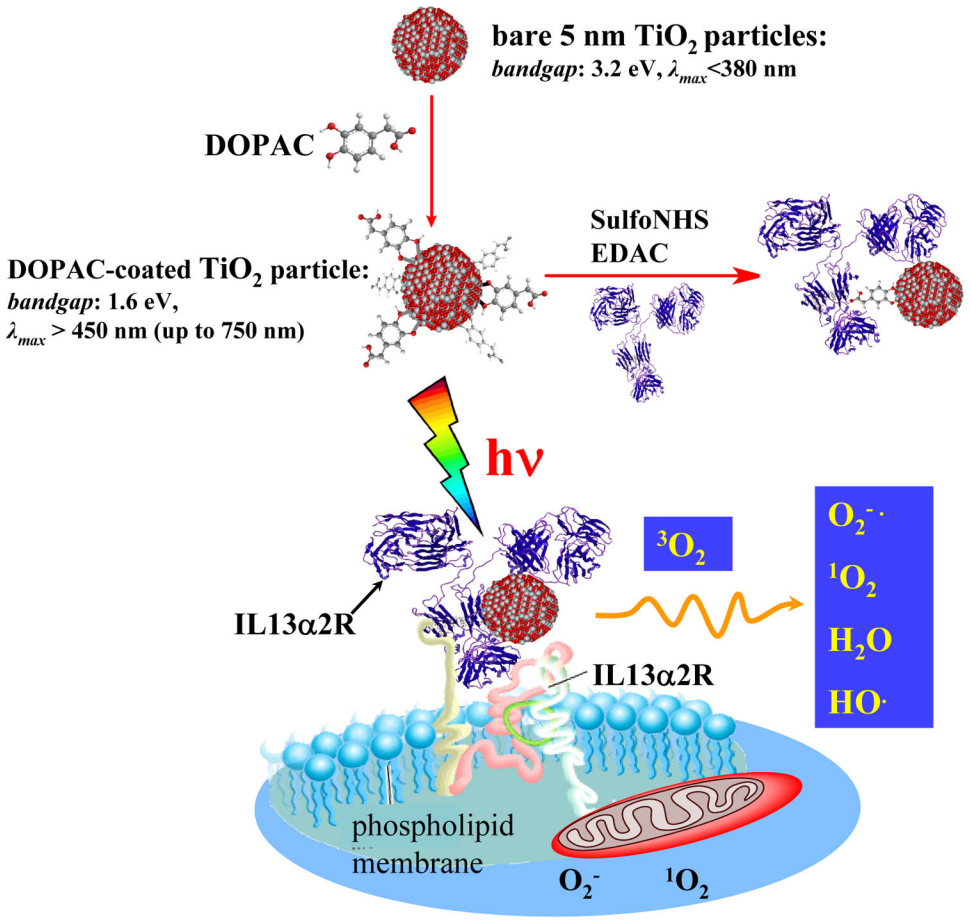

Figure 1.

General scheme. Nanobiocomposites consisted of 5 nm TiO_2 and IL13R recognizing antibody linked via DOPAC linker recognize and bind exclusively to surface IL13R. Visible light phoro-excitation of the nanobio hybrid in an aqueous solution results in formation of the various ROS. ROS, mainly superoxide cause cell membrane damage, permeability changes and cell death.

NIH-PA Author Manuscript

NIH-PA Author Manuscript

NIH-PA Author Manuscript

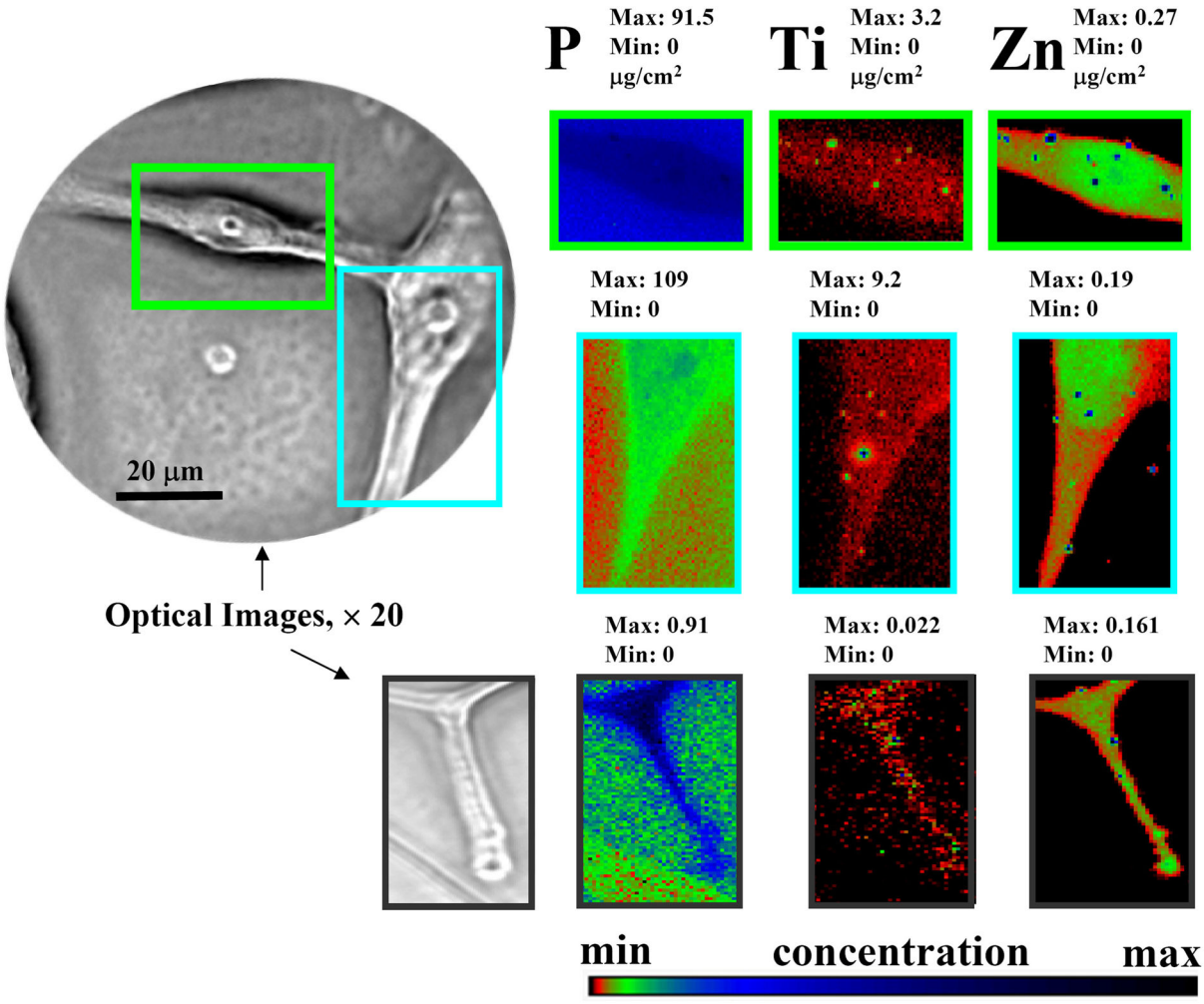

Figure 2.

X-ray fluorescence Microprobe-based visualization of the TiO_2-mAb binding to the single GBM cells (representative images of the high antigen over-expressing A172 line). Elemental distribution of biogenic phosphorous zinc are used to sketch cells and nucleus. Directed by the mAb exclusively to the surface of GB cells, TiO_2 nanoparticles spread all through the GMB cell, including cells invadopodia (lower images). The intensity of the elemental images displayed using a prism color table in logarithm scale which was shown to the bottom right. The max and minimum threshold values in micrograms per squared centimeter are given above each frame. Scans were obtained by using 10.0-keV incident energy with dwell times of 1 sec per pixel and 1-μm steps through the sample. Simultaneous appearance of intense “hot spots” in the Ti and Zn distribution images is possibly resulting of the titanium nanoparticles as well as other inorganic materials aggregation.

NIH-PA Author Manuscript

NIH-PA Author Manuscript

NIH-PA Author Manuscript

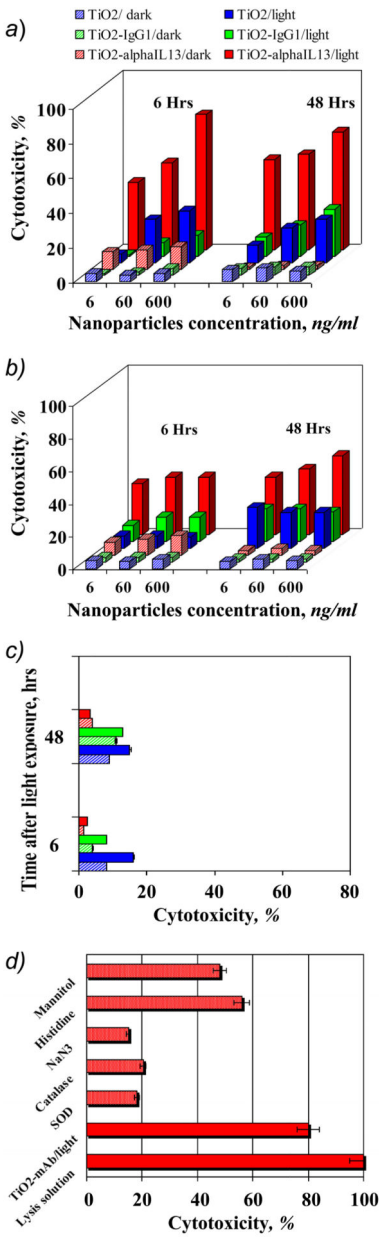

Figure 3.

Phototoxicity of the TiO_2-mAb toward A. A172 GBM cells (high ILα2R expression) B. U87 GBM cells (low ILα2R expression), C. Normal human astrocytes (NHA), and D. toward A172 cells in the presence of various free oxygen centered radical quenchers. Isotype-matched negative control antibodyl immunoglobulin IgG1, either conjugated unconjugated did not recognize isolated or cellular IL13a2R and did not show photo-induced toxicity.

NIH-PA Author Manuscript

NIH-PA Author Manuscript

NIH-PA Author Manuscript

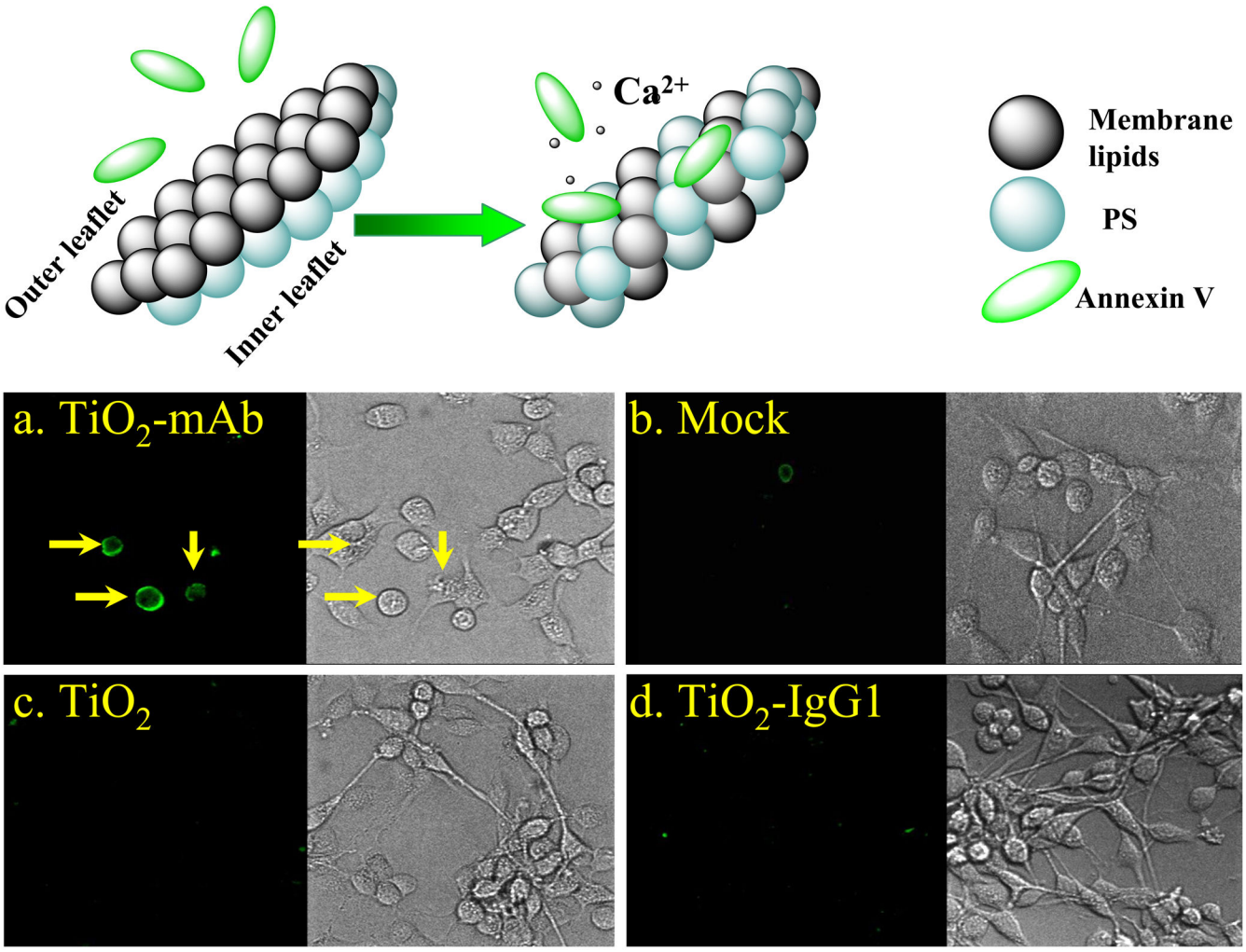

Figure 4.

Laser confocal microscopy images of the localization of Annexin V on outer membrane of the A172 GB cells after treatment with TiO_2-mAb and subsequent light exposure. After the light illumination cells were incubated for 6 hours as described in the Supporting Information, permeabilized with Triton X-100 and treated with anti-human FITC-labeled Annexin V. (a) No Annexin V distribution was observed in control experiments: (b) cells with no nanoparticles, (c) cells with bare TiO_2 particles, (d) cells with isotype-matched immunoglobulin conjugate TiO_2-IgG1.